

**STRUCTURAL, ELECTRICAL, AND OPTICAL  
PROPERTIES OF INDIUM NITRIDE THIN  
FILMS**

**UMAR BASHIR GANIE**

**UNIVERSITI SAINS MALAYSIA**

**2018**

**STRUCTURAL, ELECTRICAL, AND OPTICAL  
PROPERTIES OF INDIUM NITRIDE THIN  
FILMS**

by

**UMAR BASHIR GANIE**

**Thesis submitted in fulfillment of the requirements  
for the degree of  
Master of Science**

**April 2018**

## ACKNOWLEDGEMENT

*“All praise be to ALLAH, the most knowledgeable and wise”*

I am extremely thankful to my main supervisor, *Professor Dr Zainuriah Hassan*, for her exemplary guidance, comments, suggestions, and encouragement during my master’s degree. I also express my sincere appreciation to my co-supervisor, *Dr Naser M Ahmed*, who was always there for my guidance, suggestions, and supervision.

I am grateful to the support and cooperation from staff members of school of Physics and Institute of Nano Optoelectronics Research and Technology (INOR) at Universiti Sains Malaysia. I am also thankful to my friends and colleagues who supported me during the project.

Finally, words are not sufficient to acknowledge my beloved parents and brothers for their all-time support, encouragement, and undue love. Without their support, this study would not be possible. I specially thank my first teacher in Physics, *Mr Tariq Ahmad Mir*, who is a source of inspiration to me.

Umar Bashir Ganie

## TABLE OF CONTENTS

<b>ACKNOWLEDGEMENT</b> .....	ii
<b>LIST OF TABLES</b> .....	vii
<b>LIST OF FIGURES</b> .....	viii
<b>LIST OF SYMBOLS</b> .....	x
<b>LIST OF ABBREVIATIONS</b> .....	xii
<b>ABSTRAK</b> .....	xiv
<b>ABSTRACT</b> .....	xvi
<b>CHAPTER 1-INTRODUCTION</b> .....	1
1.1 Introduction.....	1
1.2 Motivation.....	5
1.3 Originality and novelty of work .....	5
1.4 Research objectives .....	5
1.5 Thesis outline.....	6
<b>CHAPTER 2-LITERATURE REVIEW</b> .....	8
2.1 Introduction.....	8
2.2 Early studies of InN .....	8
2.3 Thin film growth of InN .....	9
2.3.1 RF magnetron sputtering .....	11
2.4 Substrates for InN growth.....	13
2.4.1 Sapphire substrate .....	14

2.4.2	Silicon substrate .....	16
2.4.3	GaN substrate.....	17
2.4.4	Quartz substrate .....	18
2.5	Buffer layers for InN epitaxy.....	19
2.6	Physical properties of InN .....	22
2.6.1	Structural properties.....	22
2.6.2	Electrical properties .....	24
2.6.3	Optical properties.....	25
2.7	Summary.....	27
<b>CHAPTER 3-EXPERIMENTAL SETUP AND METHODOLOGY .....</b>		<b>28</b>
3.1	Introduction.....	28
3.2	RF sputtering system .....	28
3.3	Substrate cleaning.....	33
3.4	Structural characterization .....	34
3.4.1	X-ray diffraction .....	35
3.4.2	Scanning electron microscope (SEM) .....	39
3.4.3	Energy dispersive X-ray (EDX) analysis.....	42
3.4.4	Atomic force microscopy (AFM) .....	42
3.5	Optical characterization .....	44
3.5.1	Raman spectroscopy .....	44
3.5.2	Ultraviolet-visible (UV-Vis) spectroscopy .....	47
3.6	Electrical characterization .....	48
3.6.1	Hall effect measurement .....	48
3.7	Summary.....	50

**CHAPTER 4-SPUTTERED GROWTH OF InN ON SILICON, SAPPHIRE,  
BULK GaN AND QUARTZ SUBSTRATES WITH AND WITHOUT InN  
BUFFER LAYER..... 52**

4.1	Introduction.....	52
4.2	Characterization of InN films .....	52
4.2.1	XRD analysis .....	52
4.2.2	Surface morphology.....	54
4.2.3	Chemical composition .....	57
4.2.4	Surface roughness .....	58
4.3	Optical bandgap .....	61
4.4	Summary.....	64

**CHAPTER 5-SPUTTERED GROWTH OF InN ON SILICON, SAPPHIRE,  
BULK GaN AND QUARTZ SUBSTRATES USING ZnO BUFFER LAYER.. 66**

5.1	Introduction.....	66
5.2	Characterization of InN films on ZnO buffered substrates .....	66
5.2.1	Raman analysis .....	66
5.2.2	XRD analysis .....	68
5.2.3	Surface topography .....	70
5.3	Hall effect measurement .....	72
5.4	Optical bandgap .....	74
5.5	Summary.....	75

**CHAPTER 6-SPUTTERED GROWTH OF InN ON SILICON, SAPPHIRE,  
BULK GaN AND QUARTZ SUBSTRATES USING Cu DOPED ZnO BUFFER  
LAYER..... 77**

6.1	Introduction.....	77
6.2	Structural characterization .....	77

6.2.1	XRD analysis .....	77
6.2.2	Raman analysis .....	81
6.2.3	Surface topography .....	84
6.3	Optical bandgap .....	86
6.4	Hall effect measurements .....	87
6.5	Summary .....	92
<b>CHAPTER 7-CONCLUSION AND FUTURE WORK .....</b>		<b>93</b>
7.1	Conclusion .....	93
7.2	Future work.....	96
<b>REFERENCES .....</b>		<b>97</b>
<b>LIST OF PUBLICATIONS</b>		

## LIST OF TABLES

	<b>Page</b>
Table 3.1	Growth parameters for InN film and InN buffer layer..... 31
Table 3.2	Growth parameters for ZnO buffer layer ..... 31
Table 3.3	Growth parameters for InN film deposited on ZnO buffered substrates ..... 32
Table 3.4	Growth parameters for Cu-ZnO buffer layer ..... 32
Table 3.5	Growth parameters for InN film grown on Cu-ZnO buffered substrates ..... 32
Table 3.6	Raman active modes of hexagonal InN(Qian et al., 2004). ..... 46
Table 4.1	Structural parameters of as-grown InN films and on InN buffered substrates ..... 65
Table 5.1	Structural parameters of InN films grown on ZnO buffered substrates ..... 70
Table 6.1	FWHM, crystallite size, strain and lattice parameters for InN thin films grown on different substrates with Cu-ZnO buffer layer ..... 79
Table 6.2	Bond lengths, dislocation density, and unit cell volume of InN thin films grown on different substrates with Cu-ZnO buffer layer ..... 81
Table 6.3	Bandgap, surface roughness, mobility and electron concentration of InN thin films grown on different substrates with Cu-ZnO buffer layer ..... 88



## LIST OF FIGURES

		<b>Page</b>
Figure 1.1	Bandgap energy diagram of III-V nitride family with solar spectrum	3
Figure 2.1	Schematic relationship between orientations of (001) InN and c-sapphire substrate, (a) “1010 <sub>InN</sub> //1120Al <sub>2</sub> O <sub>3</sub> ”, (b) “1120 <sub>InN</sub> //1120Al <sub>2</sub> O <sub>3</sub> ” .....	16
Figure 2.2	Lattice parameters of mono and polycrystalline hexagonal InN from different studies .....	24
Figure 3.1	Flowchart of this research work .....	29
Figure 3.2	Schematic of RF sputtering system .....	31
Figure 3.3	Schematic of X-ray diffraction showing collisions between X-rays and atoms arranged in the crystal planes.....	36
Figure 3.4	Misfit dislocations between lattice mismatched film and substrate ...	38
Figure 3.5	Schematic of a SEM showing its different components.....	40
Figure 3.6	Secondary and back scattered electrons during SEM imaging.....	41
Figure 3.7	Schematic of an AFM with its components.....	43
Figure 3.8	Schematic of atomic vibrational modes in Raman spectra (Qian et al., 2004).....	45
Figure 3.9	Allowed orbital transitions in UV-Visible spectroscopy.....	48
Figure 3.10	Schematic of Hall effect .....	49
Figure 4.1	XRD patterns of InN films grown on different substrates (a) without buffer layer, (b) with InN buffer layer.....	54
Figure 4.2	Surface morphology of InN films on (a) quartz, (b) GaN, (c) sapphire, (d) Si (111) and (a`) InN buffered quartz, (b`) InN buffered GaN, (c`) InN buffered sapphire, (d`) InN buffered Si (111).. .....	56
Figure 4.3	Elemental composition of InN films on different substrates .....	58
Figure 4.4	5×5μm AFM images of as-grown films on (a) quartz, (b) GaN, (c) sapphire, (d) Si, and InN buffered substrates (A) quartz, (B) GaN, (C) sapphire, (D) Si.....	60

Figure 4.5	Reflectance spectrum of (a) as grown InN films on different substrates, (b) films grown on InN buffered substrates.....	62
Figure 4.6	Plot of RMS roughness vs Substrate .....	63
Figure 4.7	Optical bandgaps as a function of dislocation density .....	63
Figure 5.1	Raman spectra of sputtered grown InN films on ZnO buffered substrates. ....	68
Figure 5.2	XRD pattern of InN films grown on ZnO buffered substrates. ....	69
Figure 5.3	(a) variation of dislocation density and FWHM as a function of substrate, (b) variation of bond length and unit cell volume as a function of substrate .....	70
Figure 5.4	AFM image (5×5 μm) of InN films grown on ZnO buffered substrates .....	71
Figure 5.5	(a) Mobility versus Substrate, (b) Resistivity versus Substrate, (c) Carrier Concentration versus Substrate and (d) Bandgap versus Substrate. ....	73
Figure 5.6	Reflectance spectra of InN films grown on ZnO buffered substrates	75
Figure 6.1	XRD pattern of InN on different substrates with Cu-ZnO buffer layer. ....	79
Figure 6.2	(a) Variation of bond length (l) and unit cell volume as a function of substrates. (b) variation of crystallite size and electron mobility as a function of substrates.....	83
Figure 6.3	Raman spectra of InN thin films grown on different substrates.....	84
Figure 6.4	AFM images of InN thin films grown on different substrates with Cu-ZnO buffer layer. ....	85
Figure 6.5	Reflectance spectra of InN thin films grown on different substrates .	87
Figure 6.6	Percentage transmittance spectra of Cu-ZnO film on glass.....	90
Figure 6.7	(a) Change in carrier concentration as a function of electron mobility, (b) change in carrier concentration as a function of dislocation density, and (c) change in RMS roughness with respect to strain.....	91

## LIST OF SYMBOLS

$A$	Absorbance
$A$	Area
$E_g$	Bandgap
$Z$	Bending distance
$\beta$	Beta
$l$	Bond length
$\mu$	Carrier mobility
$\sigma$	Conductivity
$D$	Crystallite size
$I$	Current
$J$	Current density
$^{\circ}\text{C}$	Degree centigrade
$\delta$	Dislocation density
$N_c$	Density of states
$m_e$	Electron mass
$\mu_e$	Electron mobility
$n$	Electron/carrier concentration
$q$	Electronic charge
$F$	Force of interaction
$R_H$	Hall resistance
$V_H$	Hall voltage
$p$	Hole concentration
$m_p$	Hole mass
$\mu_p$	Hole mobility

$I$	Intensity of light reflected by sample/film
$I_o$	Intensity of light reflected by reference material
$d$	Interplanar spacing
$a, a', c$	Lattice constant
$(hkl)$	Miller indices
R	Reflectance
T	Transmittance
$h$	Planks constant
$u$	Positional parameter
$R$	Resistance
$\rho$	Resistivity
$K$	Stiffness constant
$\epsilon$	Strain
$\theta$	Theta
$V$	Unit cell volume
$c$	Velocity of light
V	Voltage
$\lambda$	Wavelength

## LIST OF ABBREVIATIONS

AC	Alternating current
AFM	Atomic force microscopy
CVD	Chemical vapor deposition
CB	Conduction band
I-V	Current-voltage
DI	Deionized
DC	Direct current
EDX	Energy dispersive X-ray
EDS	Energy dispersive X-ray spectroscopy
FWHM	Full width at half maximum
HEMT	High electron mobility transistor
HPCVD	Hybrid physical vapor deposition
IR	Infrared
KE	Kinetic energy
LD	Laser diode
L.M	Lattice mismatch
LED	Light emitting diode
LA	Longitudinal acoustic
LO	Longitudinal optic
LOPC	Longitudinal optic phonon-plasmon coupled
MFC	Mass flow controller
MOCVD	Metalorganic chemical vapor deposition
MOVPE	Metalorganic vapor phase epitaxy
MBE	Molecular beam epitaxy

NIR	Near infrared
O.T	Optical transmission
PC	Photoconductivity
PL	Photoluminescence
PLE	Photoluminescence excitation
PVD	Physical vapor deposition
PLD	Pulsed laser deposition
RCA	Radio Corporation of America
RF	Radio frequency
RF-MOMBE	Radio frequency metal organic molecular beam epitaxy
RFMBE	Radio frequency molecular beam epitaxy
RMS	Root mean square
SEM	Scanning electron microscopy
SC	Semiconductor
Sccm	Standard cubic centimeters per minute
3D	Three dimensional
TA	Transverse acoustic
TO	Transverse optic
2D	Two dimensional
UHVCVD	Ultrahigh vacuum chemical vapor deposition
UV	Ultraviolet
UV-Vis	Ultraviolet visible
WZ	Wurtzite
XRD	X-ray diffraction

# **SIFAT STRUKTUR, ELEKTRIK DAN OPTIK FILEM NIPIS INDIUM NITRIDA**

## **ABSTRAK**

InN adalah bahan yang paling kurang dikaji di kalangan III-V nitrida, disebabkan oleh cabaran yang berkaitan dengan suhu penceraian yang rendah dan kekurangan substrat yang sesuai. Penemuan jurang jalur sempit (0.7 eV) memperbaharui minat para penyelidik untuk menjalankan kajian terperinci mengenai InN untuk aplikasi optoelektronik. Teknik pertumbuhan yang biasa digunakan termasuk epitaksi alur molekul dan pemendapan wap kimia logamorganik. Percikan frekuensi radio (RF) juga biasa digunakan untuk pertumbuhan filem nipis dan nanostruktur, tetapi biasanya menghasilkan filem polihablur dengan kepekatan pembawa yang tinggi dan mobiliti elektron yang rendah. Walau bagaimanapun, faedah penggunaan percikan RF adalah ianya kaedah yang murah, mudah untuk dikendalikan dan menghasilkan filem-filem InN walaupun pada suhu bilik yang tidak mungkin didapati dengan teknik-teknik lain yang disebutkan. Kajian ini akan menggunakan percikan RF magnetron untuk pertumbuhan filem nipis InN dan mengkaji sifat struktur, elektrik, dan optik mereka. Substrat yang sering digunakan untuk pertumbuhan InN ialah Si, Al<sub>2</sub>O<sub>3</sub>, GaN dan SiC dengan ketidaksepadanan kekisi sebanyak 8%, 25%, 11% dan 15% masing-masing. Kajian ini menggunakan substrat GaN pukal, kuarza, Al<sub>2</sub>O<sub>3</sub>, dan Si (111) bagi pertumbuhan InN. Lapisan penimbal InN, ZnO, dan Cu-ZnO juga digunakan untuk melihat kesan keseluruhan terhadap pertumbuhan InN termasuk ketidaksepadanan kekisi. Pencirian struktur dilakukan menggunakan belauan sinar-X (XRD), morfologi permukaan dikaji menggunakan mikroskop imbasan elektron pancaran medan dan mikroskopi daya atomik. Spektroskopi Raman digunakan untuk mengkaji kedua-dua sifat struktur dan optik. Jurang jalur optik filem InN diperolehi menggunakan spektroskopi pantulan

ultraungu cahaya nampak. Sifat elektrik telah dikaji menggunakan pengukuran kesan Hall. Dengan penggunaan lapisan penimbal, filem InN yang bertekstur-c tinggi diperolehi atas semua substrat dengan beberapa puncak kecil dalam beberapa kes. Analisis XRD dan Raman mengesahkan bahawa filem InN adalah bersifat wurtzit heksagon. Ketidakepadanan kekisi dikurangkan antara filem InN dan substrat (Si (6.6%) dan GaN pukal (4%)) dengan penggunaan lapisan penimbal Cu-ZnO. Permukaan yang licin diperhatikan selepas penggunaan lapisan penimbal dan saiz butiran juga meningkat. Kekasaran permukaan berjulat antara 9.18 nm hingga 1.87 nm bagi InN/Si dan InN/penimbal InN/nilam masing-masing. Di antara semua kes, permukaan licin diperolehi atas substrat GaN pukal. Jurang jalur optik dilaporkan kurang daripada 2 eV. Nilai jurang jalur terendah (1.83 eV) diperolehi untuk filem InN yang ditumbuhkan atas substrat nilam dengan lapisan penimbal Cu-ZnO. Kepekatan pembawa filem InN berubah daripada  $10^{19}$ - $10^{21}$   $\text{cm}^{-3}$  untuk lapisan penimbal yang berlainan. Mobiliti filem InN meningkat apabila dimendapkan atas lapisan penimbal Cu-ZnO. Mobiliti didapati bernilai  $223 \text{ cm}^2/\text{Vs}$  atas GaN pukal,  $121.6 \text{ cm}^2/\text{Vs}$  atas silikon,  $119.2 \text{ cm}^2/\text{Vs}$  atas nilam dan  $103.7 \text{ cm}^2/\text{Vs}$  atas substrat kuarza. Kesimpulannya, filem InN dengan mobiliti yang tinggi dan kepekatan pembawa yang rendah diperolehi selepas penggunaan lapisan penimbal Cu-ZnO. Mobiliti didapati melebihi  $100 \text{ cm}^2/\text{Vs}$  atas semua substrat dengan kepekatan pembawa dalam julat  $10^{19} \text{ cm}^{-3}$ . Sebelum ini, mobiliti tertinggi bagi filem InN yang ditumbuhkan dengan kaedah percikan atas substrat nilam dengan lapisan penimbal ZnO didapati bernilai  $60 \text{ cm}^2/\text{Vs}$  dengan kepekatan pembawa  $10^{20} \text{ cm}^{-3}$ .



# **STRUCTURAL, ELECTRICAL, AND OPTICAL PROPERTIES OF INDIUM NITRIDE THIN FILMS**

## **ABSTRACT**

InN is the least studied material among III-V nitrides, due to the challenges associated with its low dissociation temperature and lack of suitable substrate. The discovery of a narrow band gap (0.7 eV) renewed the interest of researchers to carry out the detailed study of InN for optoelectronic applications. The commonly used growth techniques include molecular beam epitaxy and metalorganic chemical vapor deposition. Radio frequency (RF) sputtering is also commonly used for the growth of thin films and nanostructures, but it usually produces polycrystalline films with high carrier concentration and low electron mobility. However, the benefit of using RF sputtering are its low cost, easy to handle and produces InN films even at room temperature which is not possible with other mentioned techniques. This study will be using RF magnetron sputtering for the growth of InN thin films and study their structural, electrical, and optical properties. The commonly used substrates for InN growth are Si, Al<sub>2</sub>O<sub>3</sub>, GaN and SiC with a lattice mismatch of 8%, 25%, 11% and 15% respectively. This study uses bulk GaN, quartz, Al<sub>2</sub>O<sub>3</sub>, and Si (111) substrates for InN growth. InN, ZnO, and Cu-ZnO buffer layers were also used to see the overall effect on the growth InN including lattice mismatch. The structural characterization was carried out using X-ray diffraction (XRD) spectroscopy, surface morphology was studied using field emission scanning electron microscopy and atomic force microscopy. Raman spectroscopy was used to study both structural and optical properties. Optical bandgaps of InN films were obtained using ultraviolet-visible reflectance spectroscopy. Electrical properties were studied using Hall effect measurements. With the application of buffer layers, highly c-textured InN films

were obtained on all the substrates with some small peaks in some cases. XRD and Raman analysis confirmed that InN films are hexagonal wurtzite in nature. Lattice mismatch reduced between the InN film and substrates (Si (6.6%) and bulk GaN (4%)) with the application of Cu-ZnO buffer layer. Smooth surfaces were observed after the application of buffer layer and the grain size also increased. Surface roughness ranged from 9.18 nm to 1.87 nm for InN/Si and InN/InN buffer/sapphire respectively. Among all the cases, smooth surfaces were obtained on bulk GaN substrates. Optical bandgaps were reported to be less than 2 eV. The lowest bandgap (1.83 eV) value was obtained for InN films grown on Cu-ZnO buffered sapphire substrate. The carrier concentration of the InN films varied from  $10^{19}$ - $10^{21}$   $\text{cm}^{-3}$  for different buffer layers. The mobilities of the InN films increased when deposited on Cu-ZnO buffer layer. The mobilities were found to be 223  $\text{cm}^2/\text{Vs}$  on bulk GaN, 121.6  $\text{cm}^2/\text{Vs}$  on silicon, 119.2  $\text{cm}^2/\text{Vs}$  on sapphire and 103.7  $\text{cm}^2/\text{Vs}$  on quartz substrates. In conclusion, high mobility InN films with low carrier concentration were obtained after the application of Cu-ZnO buffer layer. The mobilities were found to be more than 100  $\text{cm}^2/\text{Vs}$  on all the substrates with a carrier concentration of the order of  $10^{19}$   $\text{cm}^{-3}$ . Previously, the highest mobility of sputtered grown InN films on ZnO buffered sapphire substrate was found to be 60  $\text{cm}^2/\text{Vs}$  with a carrier concentration of  $10^{20}$   $\text{cm}^{-3}$ .

# CHAPTER 1

## INTRODUCTION

### 1.1 Introduction

The family of III-V nitride semiconductors is represented by aluminum nitride (AlN), gallium nitride (GaN), indium nitride (InN) and their alloys like aluminum indium nitride (AlInN), gallium indium nitride (GaInN) and gallium aluminum nitride (GaAlN). Intense research has been carried out on III-V nitrides due to their potential applications in optoelectronic and photovoltaics for instance high efficiency light emitting diodes (LEDs), laser diodes (LDs) and solar cells (Veal, McConville, & Schaff, 2011). Unlike conventional III-V semiconductors, III-V nitrides are believed to be promising materials for semiconductor industry due to their important inherent features such as chemical inertness, wide bandgap, and physical hardness (Ambacher, 1998). Among III-V nitrides, most of the research has been carried out on GaN and its alloys due to their specific applications in high power and high frequency electron devices and blue/green LEDs. On the other hand, less attention was paid to InN due to its difficult growth process like low dissociation temperature, poor crystal quality, lack of suitable lattice and thermal expansion coefficient matched substrate.

The bandgap of III-V nitrides can be engineered to cover the entire visible spectrum from deep ultra violet to near infrared by alloying different compositions of III-V nitrides. Initially, InN research was not paid much attention due to its higher bandgap (1.89 eV) value. However, the research interest renewed after the discovery of new narrow bandgap (0.7 eV). The initial growth of InN by reactive sputtering and electron beam plasma techniques produced polycrystalline films (Ambacher,

1998; Osamura, Naka, & Murakami, 1975; Osamura, Nakajima, Murakami, Shingu, & Ohtsuki, 1972). Since photoluminescence (PL) emission was absent from these films, possibly due to lower crystal quality, high residual electron density, surface electron accumulation and structural defects (Zhao et al., 2012), bandgaps were measured using optical absorption, transmission, and reflectance measurements which were recorded to be 1.89 eV (Tansley & Foley, 1986b). However, the metal organic chemical vapor deposition (MOCVD) and molecular beam epitaxy (MBE) growth of InN showed a PL emission around 0.65-0.7 eV (Davydov, Klochikhin, Seisyan, et al., 2002; Wu et al., 2002). After a repeated number of attempts, the bandgap value of InN was accepted to be 0.7 eV which is much smaller than the previously reported value. With this newly observed narrow bandgap of InN, it was alloyed with GaN for making high efficiency solar cells. The bandgap of InGaN perfectly matches the solar energy spectrum with a conversion efficiency predicted to be more than 50% (Wu et al., 2002). A narrow bandgap of InN (0.7 eV) also falls in the wavelength range of optical fibers and thus provides another potential application in optical communication such as high speed laser diodes and photodiodes (Bhuiyan, Hashimoto, & Yamamoto, 2003; Monteagudo-Lerma et al., 2015). Also, the high-quality growth of InGaN/InAlN ternary alloys is used for multiple device applications such as high brightness LEDs, LDs, high electron mobility transistors (HEMTs) and photodetectors (Amirhoseiny, Hassan, & Ng, 2013b; Edmond et al., 2004; Wang et al., 2017). The invention of InGaN based blue LEDs by Nakamura et al. led them the award of 2014 Nobel prize in Physics (Nakamura, 2015). The bandgap energy diagram of nitride family is shown in Figure 1.1 (Erdoğan, Kundakçı, & Mantarcı, 2016).

Despite all these promising features, InN has received less attention as compared to AlN and GaN. This is primarily attributed to the difficulty in producing high quality InN films due to their low dissociation temperature and lack of suitable substrate. The recommended temperature for the epitaxial growth of thin films is usually equal to half of the melting point of that material.

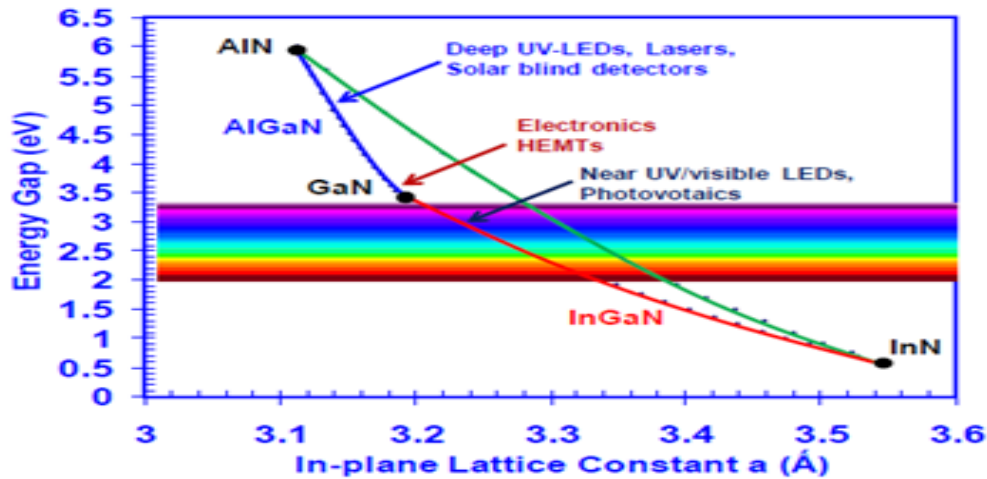


Figure 1. 1 Bandgap energy diagram of III-V nitride family with solar spectrum

The decomposition of bulk InN starts around 1373 K at a nitrogen pressure of  $10^3$  bar (Nag, 2004). The Van Vechten theory calculated the melting point of InN to be around 1900 °C, which means its growth temperature should be around 800 °C (Krukowski et al., 1998). But in practice, the dissociation of InN starts around 500 °C. which sets up an upper limit on the growth of InN films (Gallinat, Koblmüller, Brown, & Speck, 2007). Usually, high temperature growth is preferred because it provides enough kinetic energy to reactants adatoms to diffuse on the film/substrate surface. The growth rate of InN is restricted at low growth temperature and highly defective films with rough surface morphology are obtained. However, in case of InN, high temperature growth results in nitrogen atom evaporation and no In-N bond formation takes place. As a result, no film growth takes place. To prevent this, InN films should be deposited at low growth temperatures (< 500 °C). Low temperature

growth of InN is not possible with MBE, metal organic chemical vapor deposition (MOCVD), metal organic vapor phase epitaxy (MOVPE) and other techniques. The only promising technique for low temperature growth of InN is reactive sputtering.

InN is found n-type in nature due to its very high unintentional n-type doping of the order of  $10^{19}/\text{cm}^{-3}$ . The large number of dislocations and defects also limit its use in electronic devices. It was also observed that different growth methods effect the properties of InN films. Sputtered grown InN films are usually polycrystalline with high background carrier concentration. This is because, sputtering is not a controlled process which results is high oxygen/impurity incorporation. Therefore, it is difficult to produce high quality monocrystalline and hence narrow bandgap InN films with reactive sputtering. The factors which effect the bandgap of a material include deep level traps, Moss-Burstein effect, Mie resonance, oxygen incorporation, quantum confinement and nitrogen vacancies (Bagavath, Nasi, & Kumar, 2017). The reason for Moss-Burstein shift is the excessive electron carrier concentration ( $10^{19} \text{ cm}^{-3}$ ) which exceeds the conduction band edge density of states (Tansley & Foley, 1986b). Due to this, Fermi level is pushed upwards and hence lies inside the conduction band (Grundmann, 2010). Large deviations in In: N stoichiometric ratio can also result in bandgap variations. For instance, the bandgaps of nitrogen rich InN was found to be more than 2 eV. This is because, the excessive nitrogen concentration acts as a donor which results in high carrier concentration ( $10^{20} \text{ cm}^{-3}$ ) (Shrestha, Timmers, Butcher, & Wintrebert-Fouquet, 2004). The variation in the recently accepted value of 0.7-1.89 eV has been attributed to the formation of oxides in the sputtered grown films. The commonly used substrates for InN epitaxy include silicon, sapphire, silicon carbide, gallium arsenide and gallium nitride. Most of the studies have been carried out on sapphire and silicon substrates. The substrates surface morphology, polarity

and lattice mismatch greatly affect the characteristics of a film. Sometimes intermediate buffer layers are added to overcome these challenges. The commonly used buffer layers are AlN, GaN, In<sub>2</sub>O<sub>3</sub>, ZnO and sometimes the stacks of these or their alloys (Kuo et al., 2011; Laskar et al., 2011; Sato & Ito, 2011).

## **1.2 Motivation**

Although a lot of literature is available on the thin film growth of InN, but InN used in electronic devices shows a discrepancy in literature. One of the first steps for InN to be used in electronic devices is the excellent growth of a thin film. InN thin films were produced by different growth techniques mentioned in the introductory section. The motivation behind this study lies in the growth of a monocrystalline (single textured) InN film with lower optical bandgap ( $< 2$  eV) and higher carrier mobility ( $> 100$  cm<sup>2</sup>/Vs) using RF magnetron sputtering. Due to large lattice mismatch between InN and GaN, sapphire, silicon and other substrates, there is a problem to find a lattice matched substrate for InN growth, due to which the use of buffer layers is a common practice. This study will also use different buffer layers including doped buffer layer at lower growth temperatures.

## **1.3 Originality and novelty of work**

Enough research has been carried out on the growth of InN thin films using different growth methods, different substrates and buffer layers. Sputtered grown InN films were found to be high in carrier concentration ( $>10^{20}$ /cm<sup>3</sup>) and low in mobility (80 cm<sup>2</sup>/Vs). In this study, low carrier concentration and high mobility InN films using RF sputtering growth technique were obtained, which is a challenging task. Also, the use of doped buffer layers shows a discrepancy in literature. This study used Cu doped ZnO buffer layer and it was observed that the Cu doping of

ZnO buffer layer enhanced the electrical mobility of InN films on all the substrates specially on sapphire and quartz.

#### **1.4 Research objectives**

1. To investigate the effect of different substrates and buffer layers on the structural, electrical, and optical properties of InN thin films. The substrates used in this work are silicon, bulk GaN, sapphire and quartz and the buffer layers used are InN, ZnO and Cu-ZnO.
2. To enhance the electrical mobility of InN films by producing low carrier concentration films.
3. To produce InN films with optical bandgap less than 2 eV.

#### **1.5 Thesis outline**

##### **Chapter 2**

This chapter will give a detailed literature review of InN growth by different growth methods specially RF sputtering technique. The chapter will also review the structural, electrical, and optical properties of InN films carried out using different characterization techniques. Then the properties of different substrates and buffer layers used in this study will be reviewed.

##### **Chapter 3**

This chapter will discuss the methodology and theory behind this project. It will give the details of substrate cleaning procedures and then the working principle of RF sputtering and different experimental characterization tools used for InN growth.

##### **Chapter 4**



This chapter provides a discussion on the structural and optical properties of InN Thin films grown on different substrates. It is a comparative study of InN films on different substrates with and without InN buffer layer under identical conditions.

## **Chapter 5**

This chapter is a continuation of results and discussions where the structural, electrical, and optical properties of InN films grown on different substrates using ZnO buffer layer will be discussed. This chapter will discuss the simultaneous effect of different substrates and ZnO buffer layer on InN films.

## **Chapter 6**

This chapter presents the discussion on the structural, electrical, and optical properties of InN films grown on different substrates using Cu-ZnO buffer layer. This chapter is different from chapter 5 in a sense that it uses a copper (Cu) doped ZnO buffer layer.

## **Chapter 7**

This chapter presents a conclusion of the research work carried out in this thesis. The first section of this chapter sums up the results obtained in all the four steps this thesis and then suggests some potential research work to be carried out in future.

## CHAPTER 2

### LITERATURE REVIEW

#### 2.1 Introduction

In this chapter, we will focus on the literature and previous studies of InN, its growth, and physical properties. The chapter starts from a brief background of theory, early research, and growth of InN thin films. A focus will be on sputtered growth of InN because this work was carried out using RF magnetron sputtering technique. Then the issues related to InN growth, substrate, lattice mismatch, effect of substrate and buffer layer on the structural, electrical, and optical properties of InN films will be reviewed in detail.

#### 2.2 Early studies of InN

The first attempt to synthesize InN was made in 1938 using chemical decomposition of ammonium hexafluoroindate  $\text{InF}_6(\text{NH}_4)_3$  and the crystal structure was reported to be wurtzite. The synthesis of InN continued till 1972 when Hovel and Cuomo first time reported the electrical properties of polycrystalline InN films grown on sapphire and silicon substrate by RF reactive sputtering (Jain, Willander, Narayan, & Overstraeten, 2000). In Earlier 1980s, the detailed studies of InN films and their properties were carried out by Tansley and Foley using RF sputtering (Foley & Tansley, 1985, 1986; Tansley & Foley, 1984, 1986a, 1986b). Foley et al. reported the highest mobility ( $2700 \text{ cm}^2/\text{Vs}$ ) and lowest carrier concentration ( $5 \times 10^{16} \text{ cm}^{-3}$ ) of polycrystalline films at room temperature. However, different results were obtained by applying same condition by Scott et al. (Scott et al., 2001). They reported a mobility of less than  $100 \text{ cm}^2/\text{Vs}$  with a carrier concentration of the order of  $10^{19} \text{ cm}^{-3}$ . Only recently, InN film with a record high mobility of  $3280 \text{ cm}^2/\text{Vs}$  and

carrier concentration of  $1.47 \times 10^{17} \text{ cm}^{-3}$  was reported (Wang et al., 2012). Based on absorption and transmittance results, the bandgap of InN was reported to be 1.89 eV as mentioned earlier in section 1.1. This bandgap value was accepted for more than a decade until 2002. This band gap value became one of the reasons for less attention paid to InN research because this bandgap range was already covered by some other good materials such as AlGaAs and InGaP (Kruse, Einfeldt, Böttcher, & Hommel, 2001; Neugebauer et al., 2003).

### **2.3 Thin film growth of InN**

Despite its promising features and potential applications in semiconductor industry, the growth process of InN halts its progress for full realization. The main factors responsible for the difficult growth of InN are low dissociation temperature which starts around 500°C (Gallinat et al., 2007), lack of suitable lattice matched and thermal coefficient matched substrate and high nitrogen vapor pressure. The nitrogen partial pressure was reported to be main factor for InN thermal equilibrium (Trainor & Rose, 1974). When annealed above 500°C, the decomposition starts within a short time and leaves a residue of indium in nitrogen. On the other hand, when InN was heated at low nitrogen pressure of  $10^{-3}$  Torr, the InN sample sustained at 500°C. Trainor et al. (Trainor & Rose, 1974) also mentioned that high quality InN films could be produced at higher temperatures using lower pressure and growth rates. In 1977, chemical vapor deposition growth of InN was first time reported with a dissociation temperature of 600°C (Marasina, Pichugin, & Tlaczala, 1977). In 1990, Wakahara et al. produced single texture InN film on sapphire (0001) substrate at a temperature range of 400- 600°C using microwave-excited metalorganic vapor phase epitaxy (MOVPE). They reported the growth of InN film along (002) plane (Wakahara, Tsuchiya, & Yoshida, 1990).

Other methods used to produce InN include molecular beam epitaxy (MBE), metalorganic chemical vapor deposition (MOCVD), pulsed laser deposition (PLD), and RF sputtering (Ivanov et al., 2004; Nanishi, Saito, & Yamaguchi, 2003; Tuna et al., 2011; Valdueza-Felip et al., 2012). So far, MBE and MOCVD have proved to be efficient methods for producing single crystal InN films. However, the epitaxial growth in low pressure systems like that of MBE and MOCVD is difficult due to its low dissociation temperature and further, equilibrium pressure of nitrogen increases with increase in deposition temperature (Davydov & Klochikhin, 2004). It is very difficult to produce good quality InN films with these methods at low temperatures. This is because, at low temperatures, the migration of adatoms is slow and the reactants kinetic energy is not enough to produce a well coalesced structure. Apart from this, these methods are very costly. RF sputtering is one of the first techniques for crystal growth. It produces both non-crystalline and crystalline films. Moreover, RF sputtering can produce good quality films at low temperatures even at room temperature, which is not possible with other techniques. Therefore, for InN, which starts dissociating at 500 °C, RF sputtering can be used to produce good quality films at low temperatures. Sputtered growth of InN on sapphire, silicon, glass and silicon carbide substrates has already been reported (Ambacher, 1998; Amirhoseiny, Hassan, Ng, & Ahmad, 2011; Amirhoseiny, Hassan, Ng, & Alahyarizadeh, 2013; Da Silva et al., 2012). Bulk GaN has emerged as a promising material for semiconductor industry. It is used both as substrate as well as epitaxial growth. Here bulk GaN will be used as a substrate for InN growth due to its excellent electrical properties. We will also use quartz substrate, which is available in best quality with low price. It is a challenge to produce good quality InN films on quartz due to its amorphous nature.

So far, no high mobility InN films have been produced on quartz substrate using RF sputtering technique.

### **2.3.1 RF magnetron sputtering**

Depending on the materials characteristics, substrates, precursors, and growth parameters, there are two deposition methods that scientists and engineers have been using for crystal and thin film growth namely physical vapor deposition (PVD) and chemical vapor deposition (CVD). The physical vapor depositions include MBE, sputtering and pulsed laser deposition (PLD) and chemical vapor deposition includes MOCVD, Hybrid Physical & Chemical Vapor Deposition (HPCVD), and Ultra High Vacuum chemical vapor deposition (UHVCVD). Here, RF sputtering will be used for InN growth. One of the advantages of sputtering technique is, it is used for large area growth of thin films at low temperatures and low costs. Sputtering technique is used when growth is performed either at room temperature or below 400°C.

In sputtering, a target material acts as a precursor for film growth. Particles are ejected from this solid target material after bombardment with energetic ions which are produced by chamber plasma. The ions strike the target with high kinetic energies and eject the target material which then lands on the substrate and forms a film. Since there is no change in substrate target distance during deposition, no change in substrate and target angle, no relative motion between the substrate and target. Therefore, it is easy to operate and produces a film of uniform thickness (Behrisch). Two kinds of sputtering techniques are usually used, if the voltage supply is direct current (DC), then it is called DC sputtering and if the voltage supply is alternating current (AC), then it is called RF sputtering. DC sputtering is used for conductive targets like metals. However, its limitation is that, it cannot be used for

non-conducting and insulating materials. This is because, the ions of the chamber land on the target material which attains positive charge and hence sputtering won't take place. On the other hand, RF sputtering can be used for both insulating and conductive materials. Because here the AC current alternates the potential of the current at radio frequency producing positive and negative cycles and hence charge buildup won't take place. In RF sputtering, the target acts as a cathode and the substrate as anode. When the plasma is created inside the chamber, the positive charged ions with sufficient kinetic energy strike the target material (cathode), this ejects the target particles which move towards the substrate surface and deposit as a film. In case of reactive sputtering, the reactant gas used, apart from inert argon gas, reacts with the adatoms and land on the substrate. In case of InN, the indium adatoms react with nitrogen atoms in the chamber and form InN, which is then deposited on the substrate (Mattox & Mattox, 2003).

Sputtering was the first technique used for InN growth. The detailed mechanism about the reactive sputtering and growth of InN in Ar-N<sub>2</sub> ambient is demonstrated by Natarajan et al. (Natarajan, Eltoukhy, Greene, & Barr, 1980). Many attempts were made to upgrade the technique and some studies report the growth of single crystalline InN films as well. However, overall film qualities were poor with high background carrier concentration of the order of  $10^{20}$  cm<sup>-3</sup> with mobilities less than 100 cm<sup>2</sup>/Vs (A. G. Bhuiyan et al., 2003). However, recently, some groups have reported the high quality sputtered growth of InN thin films on silicon and GaN substrates (Q. Guo, Ogata, Ding, Tanaka, & Nishio, 2009; Harotoonian & Woodall, 2016; Valdueza-Felip et al., 2011).

## 2.4 Substrates for InN growth

After the development of a new material, one of the most important requirements to study its properties is a suitable substrate. If the materials substrates are not available in bulk, a lattice matched foreign substrate is used as an alternative. In case of InN, the research has not matured so much that bulk substrates can be produced. People are still studying its properties to use it in industry. Therefore, heteroepitaxy of InN on different substrates have been going on from last two decades. In the earlier research on InN, sapphire was the most commonly used substrate due to its wide availability, hexagonal symmetry, and ease in pre- growth cleaning. However, the large lattice mismatch of 25% between InN and sapphire produces misfit dislocations which affects the structural, electrical, and optical properties of InN based devices (Jain et al., 2000). Apart from sapphire, other substrates used for InN growth are silicon (Si), silicon carbide (SiC), gallium arsenide (GaAs), gallium phosphide (GaP), magnesium aluminate (MgAl<sub>2</sub>O<sub>4</sub>), yttria-stabilized zirconia (YSZ), germanium (111) (Ge), glass and gallium nitride (GaN) (Amirhoseiny, Hassan, & Ng, 2013a; Amirhoseiny et al., 2011; Amirhoseiny, Hassan, Ng, et al., 2013; A. Bhuiyan, Yamamoto, & Hashimoto, 2001; Fareed et al., 2004; Ive et al., 2004; Murakami et al., 2008; T. Nakamura, Tokumoto, Katayama, Yamamoto, & Onabe, 2007; Trybus et al., 2005; Tsuchiya et al., 2000; Zhi et al., 2012). The lattice mismatch between Si and InN is 8%, but nucleation and growth of InN on Si requires an AlN buffer/intermediate layer. Also, Si has a great tendency to react with precursors to form SiN, SiAl and in case of sputtering, SiO<sub>2</sub>, which forms an unintentional buffer layer on the substrate and hence affects proper growth of InN on Si. Although, the lattice mismatch between SiC and InN is lower (15%) as

compared to sapphire but the higher cost of SiC substrate makes it less preferable in device industry.

Research on InN growth on many other substrates has been carried out but there are limitations with every material like cost, chemical and thermal stability, lattice and thermal coefficient mismatch, wide availability of high quality substrates at cheaper prices etc. Therefore, no ideal substrate has been decided yet. However, the preferable substrates used for InN growth are sapphire, Si and GaN. This is because, the growth of other nitrides on these substrates has produced very good results and hence emphasis is on high quality InN growth on these substrates. Another reason is the wide usage of these substrates in industry and therefore integration of InN is easy. Although, InN growth on glass substrates have shown poor results but due to their wide availability in high quality and cheaper prices, quartz substrates will also be used in this study.

#### **2.4.1 Sapphire substrate**

As mentioned above, the use of sapphire substrate is very common in InN epitaxy due to its wide availability at low price. The large lattice and thermal coefficient of expansion mismatch results in high density of structural defects. However, studies show that surface pretreatment, surface nitridation and application of a buffer layer improves the film quality. Initially, AlN buffer layer was used which showed great enhancement in structural properties due to a reduced lattice mismatch of 13%. The insertion of InN and GaN buffer layers also showed a great improvement in structural, electrical, and optical properties of InN films. Generally, the structure of InN grown on sapphire is hexagonal wurtzite with a few reports of cubic InN. Cimalla et al. (Cimalla et al., 2004) reported the direct growth of cubic



InN on r-plane sapphire and Lozano et al. (Lozano, Morales, Garcia, Gonzalez, et al., 2007) fabricated cubic InN on (0001) sapphire using cubic In<sub>2</sub>O<sub>3</sub> as buffer layer. The reports about the epitaxial relationship between InN and sapphire vary, depending upon the pre- growth treatment and substrate orientation. For instance, InN grown on c-plane sapphire shows parallel orientation while as the InN grown on nitrided sapphire,  $\alpha$ -sapphire or AlN, GaN buffer layers show “[10 $\bar{1}$ 0]<sub>InN</sub>//[10 $\bar{1}$ 0]<sub>AlN</sub>//[11 $\bar{2}$ 0]<sub>Al<sub>2</sub>O<sub>3</sub></sub>” epitaxial relation. However, when InN is directly grown on  $\alpha$ -sapphire, without surface treatment and buffer layer, it shows either “[10 $\bar{1}$ 0]<sub>InN</sub>//[11 $\bar{2}$ 0]<sub>Al<sub>2</sub>O<sub>3</sub></sub>” or “[11 $\bar{2}$ 0]<sub>InN</sub>//[11 $\bar{2}$ 0]<sub>Al<sub>2</sub>O<sub>3</sub></sub>” epitaxial relations depending on the growth process. Figure 2.1 (Guo, Yamamura, Yoshida, & Itoh, 1994) shows the schematic relationship between InN and sapphire substrate in both the above-mentioned relationships. It was also reported that growth temperature plays a dominant role in determining the epitaxial relationship between InN film and sapphire substrate (Cimalla et al., 2003; Lozano, Morales, Garcia, González, et al., 2007; Pan et al., 1999; Tsuchiya, Yamano, Miki, Wakahara, & Yoshida, 1999; Yamamoto, Tsujino, Ohkubo, & Hashimoto, 1994b).

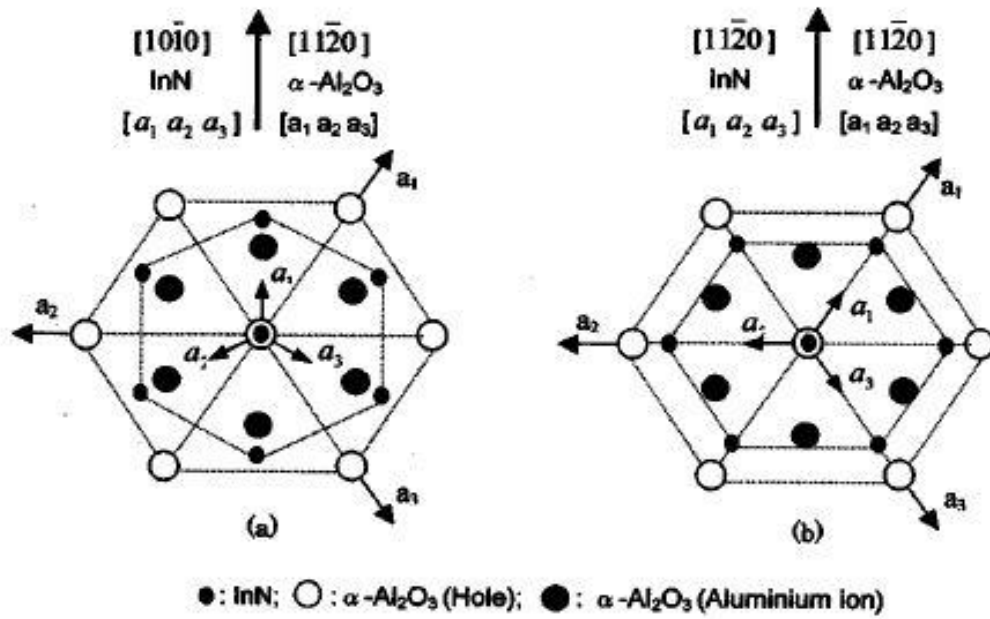


Figure 2. 1 Schematic relationship between orientations of (001) InN and c-sapphire substrate (a) “ $[10\bar{1}0]_{\text{InN}}//[11\bar{2}0]_{\text{Al}_2\text{O}_3}$ ”, (b) “ $[11\bar{2}0]_{\text{InN}}//[11\bar{2}0]_{\text{Al}_2\text{O}_3}$ ”

#### 2.4.2 Silicon substrate

Since silicon is the most widely used substrate in semiconductor industry, therefore, it was also widely used for InN growth. The first time Si was used as a substrate for InN based solar cell was in 1994 by Yamamoto et al. (Yamamoto, Tsujino, Ohkubo, & Hashimoto, 1994a). He reported that the direct growth of InN on Si did not take place, it instead formed a SiN buffer layer due to unintentional nitridation of substrate surface. The growth was carried out at a temperature of 400°C or below. It was observed that the substrate nitridation takes place even at lower temperatures and results in polycrystalline film due to reduced migration of adatoms. To prevent the formation of SiN buffer layer, a GaAs buffer layer was first deposited on Si substrate followed by the growth of InN epilayer. Later, MBE, MOCVD and MOVPE reported direct growth of InN on Si (Grandal & Sánchez-García, 2005;

Jamil et al., 2008; Sánchez-García et al., 2006). However, the direct growth of monocrystalline InN on Si at lower temperatures still remains a challenge. This study carried out the direct growth of InN on Si as well as on buffered Si substrates at lower temperatures.

### **2.4.3 GaN substrate**

The realization of a blue LED by Akasaki, Amano and Nakamura has proved that GaN is one of the excellent materials for device growth. Apart from their excellent optical properties, GaN shows high thermal conductivity, excellent electron transport and high breakdown voltage. Besides, the saturation velocity of GaN is higher than other conventional semiconductors. This is because of the large energy separation between electrons in conduction band  $\Gamma$  and L valleys. This large energy separation of electrons in GaN based devices suppresses the intervalley transitions under the application of high electric field. Therefore, GaN based devices can achieve high power and high frequency operations owing to their excellent material properties (Ueda, 2017). Lu et al. first time reported the highest mobility and lowest carrier concentration on InN films grown on bulk GaN substrates using MBE growth technique. The mobility was reported to be  $2050 \text{ cm}^2/\text{Vs}$  with a carrier concentration of  $3.493 \times 10^{17} \text{ cm}^{-3}$  (Bhuiyan et al., 2003). Yamaguchi et al. reported the high-quality growth and mobility of InN on GaN substrates using MOVPE. They also reported that the insertion of a GaN buffer layer improved the structural properties significantly and reduced the defects in InN films (Yamaguchi et al., 1999). The polarity of GaN substrates has also great impact on the properties of InN film. For instance, at room temperature, an InN film grown on N face GaN showed a mobility of  $800 \text{ cm}^2/\text{Vs}$  with a carrier concentration of  $2.1 \times 10^{19} \text{ cm}^{-3}$  (Wang, Che, Ishitani, & Yoshikawa, 2006; Xu et al., 2003). It was also reported that InN grown on GaN

template by MOVPE above 550°C shows more indium content as compared to other substrates. This was attributed to surface polarity of GaN and InN (Yamaguchi et al., 1999). Therefore, to realize the high quality and high mobility InN growth on GaN substrates, high quality GaN substrates are needed. So far, high quality GaN substrates have been achieved. Therefore, GaN substrates can prove ideal for InN growth.

#### **2.4.4 Quartz substrate**

Glass is the cheapest material among all other materials used as substrates for device and film growth. Quartz, a form of glass was also used by researchers for thin film growth but due to poor results, it was not given much attention. However, it is still being used for some transparent materials growth like ZnO and ITO for photovoltaic applications (O'Dwyer et al., 2009; Rusop, Uma, Soga, & Jimbo, 2006). Iwata et. al reported the growth of GaN on glass and sapphire substrates and carried out the comparative study. They reported a strong emission peak and (002) oriented n-type GaN film on fused silica glass substrate with a carrier concentration of  $7 \times 10^{16} \text{ cm}^{-3}$  and a mobility of  $23 \text{ cm}^2/\text{Vs}$  (Iwata, Asahi, Asami, Kuroiwa, & Gonda, 1997). Inoue et al. (Inoue, Namazu, Suda, & Koterazawa, 2004) reported the sputtering growth of highly c-textured InN on glass substrate with an angular dispersion of  $3^\circ$ . These values are better than the ones reported on ZnO buffered sapphire substrates by Ikuta et al. (Ikuta, Inoue, & Takai, 1998). Moreover, unintentional growth of any oxide or nitride buffer layers have been rarely reported on quartz/glass substrates unlike sapphire and silicon. Therefore, in this study quartz substrates will be used as a substrate for InN growth and different buffer layers will also be applied to ensure better crystal quality.

## 2.5 Buffer layers for InN epitaxy

The use of buffer layers or two-step growth process for heteroepitaxial growth is now commonly used in thin film crystal growth. Results have proven that the application of buffer layers reduces the lattice mismatch and thermal coefficient of expansion mismatch between the film and substrate and hence reduces the strain between the two. A buffer layer is a thin layer which is deposited on a bare substrate at lower temperatures as compared to epilayer. This is followed by the growth of a main epilayer on this already deposited buffered substrate. That is why it is called a two-step growth process. The main epilayer is usually thicker than the buffer layer and is more often deposited on higher temperatures than buffer layer. The buffer layer promotes the growth of main epilayer due to the induction of high density of nucleation centers. The application of a buffer layer reduces the free energy of the system due to 3D island growth at lower temperatures. This happens because of the large difference between the lattice constant of substrate and buffer layer. It is observed that the 3D islands of the buffer layer are coherent with the substrate and the ramping time and annealing of the buffer layer greatly affects its structural properties and hence the subsequent growth of main epilayer. A lot of work has been done on the two-step growth of GaN but in case of InN, two-step growth has been carried out by MBE and MOVPE techniques. There is not enough work on the two-step growth of sputtered grown InN films. In one of the earlier works, Mamutin et al. (Mamutin et al., 1999) reported the high-quality MBE growth of InN films on sapphire substrate. The growth was carried out on a 15-nm thick InN buffer layer which was annealed at high temperature. Saito et al. (Yoshiki Saito, Teraguchi, Suzuki, Araki, & Nanishi, 2001) carried out the growth of high mobility InN on low temperature grown InN buffer layer, annealed at higher temperatures. They also

reported the application of a low temperature buffer layer produces high quality InN films. The room temperature electron mobility of the InN films was  $830 \text{ cm}^2/\text{Vs}$  with a carrier concentration of  $1.0 \times 10^{19} \text{ cm}^{-3}$ . While as the mobility of InN films grown without buffer layer was reported to be  $150 \text{ cm}^2/\text{Vs}$  with a carrier concentration of  $4.2 \times 10^{20} \text{ cm}^{-3}$  (Yoshiki Saito et al., 2001). Lu et al. (Lu et al., 2001) reported that the application of an AlN buffer layer significantly enhances the structural and electrical properties of InN film. They showed that as the thickness of AlN buffer layer increases, the electrical mobility of InN film increases monotonically, and the carrier concentration decreases. They also reported an improvement in the surface morphology of InN films. More importantly, they showed that if grown under optimum conditions, an MBE grown InN grown on AlN buffer layer will be of similar quality compared to the InN grown using migration-enhanced epitaxy (Yamaguchi, Kawashima, & Horikoshi, 1988). This result strongly suggests that the quality of the InN film does not depend on the growth method alone but also strongly depends on the quality of the buffer layer and surface morphology. Higashiwaki et al. (Higashiwaki & Matsui, 2002) reported a significant improvement in the structural and electrical properties of InN film with the application of a low temperature InN and GaN buffer layer. They showed that a low temperature stack of InN and GaN buffer layer is more effective than a low temperature InN buffer layer alone. They reported the room temperature mobility of  $545 \text{ cm}^2/\text{Vs}$  with a carrier concentration of  $5.5 \times 10^{18} \text{ cm}^{-3}$  for an InN film grown on InN buffer layer. While as, for an InN film grown on the stack of InN and GaN, the room temperature mobility was reported to be  $1420 \text{ cm}^2/\text{Vs}$  with a carrier concentration of  $1.4 \times 10^{18} \text{ cm}^{-3}$ . Cheng et al. (Shih, Lo, Pang, & Hsieh, 2010) reported the plasma assisted molecular beam epitaxy (PAMBE) growth of InN on  $\text{In}_2\text{O}_3$  buffered ZnO substrate. They observed that due to

the reaction of In with O, an  $\text{In}_2\text{O}_3$  compound formed between the film and the substrate which subsequently formed pits in the InN epilayer layer when directly grown on ZnO substrate. However, the pits disappeared when an  $\text{In}_2\text{O}_3$  buffer layer was intentionally deposited before the growth of InN main layer. Yusato et al. (Sato & Ito, 2011) reported the growth of InN and InGaN films on  $\text{In}_2\text{O}_3$  buffer layer on sapphire substrate and reported the structural enhancement in InN films grown on  $\text{In}_2\text{O}_3$  buffer layer as compared to the InN grown without buffer layer. In a recent study, Shou et al. (Kuo et al., 2011) reported the growth of hexagonal InN by radio frequency molecular beam epitaxy (RFMBE) on low temperature grown ZnO buffer layer on sapphire substrate. They reported the room temperature mobility of  $165 \text{ cm}^2/\text{Vs}$  with a background carrier concentration of  $2.0 \times 10^{20} \text{ cm}^{-3}$ . Pan et al. (Pan et al., 1999) reported the two-step growth of MOVPE grown InN film on low temperature InN buffer layer. They did not get any significant improvement in the results and hence concluded that the two-step growth is not suitable in MOVPE systems. Guo et al. (Guo, Kato, & Yoshida, 1993) reported the decomposition of a single crystalline InN film when annealed above  $550^\circ\text{C}$  in nitrogen ambient which damaged the surface morphology of the film due to nitrogen evaporation. Lascar et al. (Laskar et al., 2011) reported the MOVPE growth of InN on different buffer layers namely InN, AlN and GaN on sapphire substrate under identical conditions. They showed that the best structural, electrical, and optical results were produced by AlN buffer layer. The mobility was found to be 111, 234 and  $342 \text{ cm}^2/\text{Vs}$  with a carrier concentration of  $1.43 \times 10^{19}$ ,  $1.39 \times 10^{19}$  and  $0.68 \times 10^{19} \text{ cm}^{-3}$  for InN, GaN and AlN buffer layer respectively. Zhang et al. carried out the MOCVD growth of InN on GaN and InN buffered sapphire substrates (Zhang et al., 2011). They varied the temperature of buffer layers and showed that GaN buffer grown at  $800^\circ\text{C}$

significantly improved the crystal quality of InN epilayer as compared to the GaN buffer deposited at 550 °C. However, they did not observe any significant change in crystal quality of InN film when deposited on low temperature InN buffer layer. Based on the above results, we can conclude that buffer layers strongly affect the InN film properties and produces better results.

Many results were not found on the sputtered growth of InN using buffer layers. This may be because, sputtering was one of the earlier techniques used for InN epitaxy. After that other advanced methods were used. One of the earlier studies shows the sputtered growth of InN thin film on ZnO buffered sapphire substrate (Ikuta et al., 1998). They reported an improved structural quality of InN films on ZnO buffer layer with an electron mobility of  $60 \text{ cm}^2/\text{Vs}$ , which is twice the InN films deposited on bare substrates, with a carrier concentration of  $2.0 \times 10^{20} \text{ cm}^{-3}$ , while as the carrier concentration of InN films grown on bare substrates was found to be  $3.0 \times 10^{20} \text{ cm}^{-3}$ . Monteagudo et al. (Monteagudo-Lerma et al., 2016) recently reported the sputtered growth of InN nanostructures on InN and AlN buffer layers on sapphire substrates. They showed that the “column density and diameter” strongly depend on the morphology and growth parameters of buffer layer. They reported that, in terms of mosaicity, best results were obtained on AlN buffer layer. The above studies show that most of the work has been done on sapphire substrate, with some few studies on buffered Si and GaN. No study was reported on buffered quartz substrates. This study will study the effect of different buffer layers including doped buffer layer on sputtered grown InN on different substrates namely sapphire, Si, bulk GaN and quartz.

## **2.6 Physical properties of InN**

### **2.6.1 Structural properties**



The crystalline structure of InN was first studied by Juza and Hahn (Juza & Hahn, 1938). They reported that InN exists in wurtzite hexagonal structure with lattice parameters  $a = 3.53 \text{ \AA}$  and  $c = 5.69 \text{ \AA}$ . However, Kubota et al. (Kubota, Kobayashi, & Fujimoto, 1989) reported different values of lattice parameters  $a = 3.540 \text{ \AA}$  and  $c = 5.705 \text{ \AA}$  for sputtered grown polycrystalline InN. Davydov et al. (Davydov, Klochikhin, Seisyan, et al., 2002) reported the high quality growth of monocrystalline InN films with lattice parameters  $a = 3.5365 \text{ \AA}$  and  $c = 5.7039 \text{ \AA}$ . Figure 2.2 shows the lattice parameters of mono and polycrystalline hexagonal InN reported in different studies. The graph shows variations in lattice parameters from theoretically reported values. This may be due to the structural defects and incorporation of impurities in the crystal (Hoffmann, 2003). InN also exists in zinc blende structure. Strite et al. (Strite et al., 1993) reported the growth of zinc blende InN on GaAs substrate with a lattice parameter of  $4.98 \text{ \AA}$  while as other study (Lima et al., 1999) reported the lattice constant to be  $5.04 \text{ \AA}$  as measured by ‘reflection high energy electron diffraction’. Many studies have reported that the structure of InN depends on multiple factors which includes substrate, growth technique, film thickness, buffer layer, temperature etc. For instance, InN films with a thickness of less than  $1200 \text{ \AA}$  form 3D grain islands having different crystalline orientation. It was also observed that due to change in growth mode, screw dislocations begin to appear at a thickness of  $1200 \text{ \AA}$ .

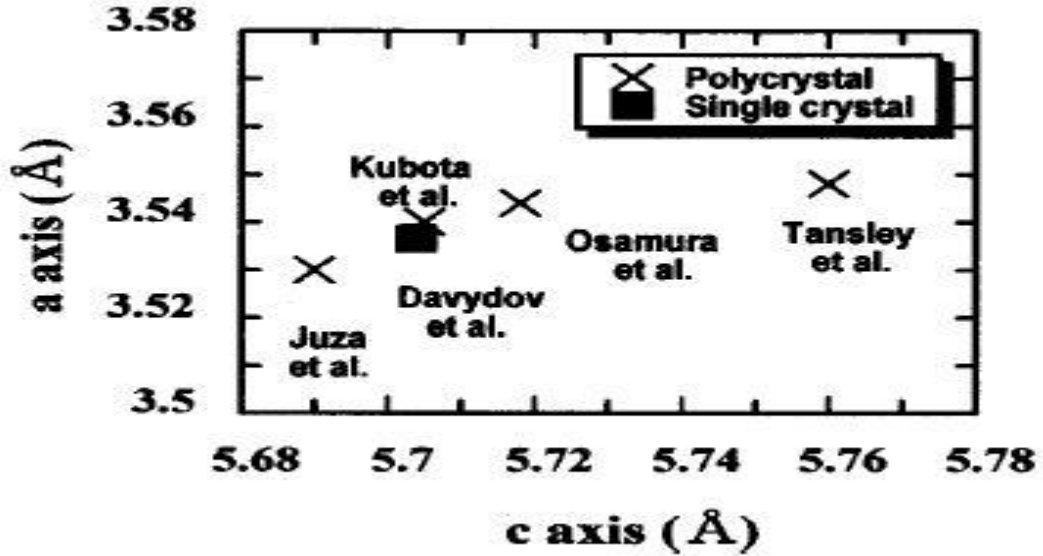


Figure 2.2 Lattice parameters of mono and polycrystalline hexagonal InN from different studies

## 2.6.2 Electrical properties

Intrinsic InN is found n-type in nature having a very high background carrier concentration. Jones et.al (Jones et al., 2006) reported the first p-type doping of InN with magnesium (Mg) doping. Recently, Guo et al. (Guo et al., 2014) reported the n-p type transition of Mg doped InN using “photoconductivity (PC) and thermopower measurements”. The initial growth of InN was mostly carried out by RF sputtering technique. The sputtered grown InN films were polycrystalline with a carrier concentration of the order of  $10^{18}$  to  $10^{21}$   $\text{cm}^{-3}$  with a mobility ranging from 20 to 250  $\text{cm}^2/\text{Vs}$ .

However, an exceptional study carried out by Tansley and Foley showed a drastically decreased carrier concentration of  $5 \times 10^{16}$   $\text{cm}^{-3}$  and a high electron mobility of 2700  $\text{cm}^2/\text{Vs}$  (Tansley & Foley, 1984). No other studies reported such a high mobility when prepared under same conditions. These studies reported InN films with very high carrier concentrations of the order of  $10^{20}$   $\text{cm}^{-3}$  and an electron